frontiers | Frontiers in Marine Science

TYPE Original Research
PUBLISHED 11 January 2024
DOI 10.3389/fmars.2023.1276028

OPEN ACCESS

EDITED BY
Selvaraj Kandasamy,
Central University of Tamil Nadu, India

REVIEWED BY
Fajin Chen,
Guangdong Ocean University, China
Jin-Yu T. Yang,
Xiamen University, China

*CORRESPONDENCE
Dong-Jin Kang
djocean@kiost.ac.kr

RECEIVED 11 August 2023
ACCEPTED 27 December 2023
PUBLISHED 11 January 2024

CITATION
Kim Y and Kang D-J (2024) Oxygen isotopic fractionation during dissolved oxygen consumption in the bottom layer of the Ulleung Basin, East/Japan Sea.
Front. Mar. Sci. 10:1276028.
doi: 10.3389/fmars.2023.1276028

Oxygen isotopic fractionation during dissolved oxygen consumption in the bottom layer of the Ulleung Basin, East/Japan Sea

Yeseul Kim[1] and Dong-Jin Kang[2,3]*

[1]Marine Environmental Research Department, Korea Institute of Ocean Science and Technology (KIOST), Busan, Republic of Korea, [2]Korea Institute of Ocean Science and Technology (KIOST) School and Academic Programs Division, Korea Institute of Ocean Science and Technology (KIOST), Busan, Republic of Korea, [3]Department of Ocean Science, University of Science and Technology (UST), Daejeon, Republic of Korea

The interpretation of decline in dissolved oxygen (DO) in the oxygenated bottom water of the Ulleung Basin (UB), southwest of the East/Japan Sea has been challenging because of the integrated influence of various DO-consuming processes. Therefore, the stable oxygen isotopic fractionation of DO was investigated to enhance our understanding of the distinct DO consumption observed in the bottom layers of the center of the UB. We explored the relationship between DO and its oxygen isotope composition ($\delta^{18}O_{DO}$) using data collected at a station located in the center of the UB in 2020, 2021, and 2022. An unforeseen decrease in $\delta^{18}O_{DO}$ in the bottom layer (> 1800 m) where DO was depleted was discovered. The overall DO consumption in the mesopelagic water layer (300–1000 m), primarily attributed to water column respiration, exhibited an isotopic fractionation factor (α) with 0.985 ± 0.001 in the $\delta^{18}O_{DO}/[O_2]$ relationship. The consumptive isotope fractionation factor in the bottom waters near the sediments (approximately 2146 m) showed a value slightly higher (0.988 ± 0.002) than that in the mesopelagic water layer. This isotopic signature is likely due to a smaller fractionation in the bottom waters relative to the mesopelagic water. The isotopic evidence suggests the involvement of mineral oxidation associated with excess dissolved Mn and Fe in the bottom waters because mineral oxidation exhibits a smaller fractionation effect than respiration. Our study demonstrates that DO depletion results from multiple consumption processes, including respiration, mineral oxidation, and diffusive transport, and the isotopic behavior provides evidence that mineral oxidation significantly influences DO consumption.

KEYWORDS

dissolved oxygen, oxygen depletion, multiple consumption factors, oxygen isotopic composition, Ulleung Basin, East/Japan Sea

1 Introduction

Dissolved oxygen (DO) is a crucial field parameter because it is a key factor in evaluating metabolic activity and ecological health in marine ecosystems and is the most readily available oxidizing agent (Hobbs and McDonald, 2010). There are various factors controlling the DO content as sources and sinks (Hanson et al., 2008; Bocaniov et al., 2012), including gas exchange, photosynthesis, respiration, and other small but significant processes (Lee et al., 2003; Wassenaar and Hendry, 2007), such as mineral interactions, diffusive transport, and biochemical reactions. In addition, the distribution of DO in the ocean interior is influenced by physical processes such as ocean circulation (Joos et al., 2003; Zuo et al., 2019). Therefore, biogeochemical and physical processes are crucial factors that affect oxygen budgets in ocean environments. In general, understanding the spatial and temporal contents of DO is challenging because they are simultaneously affected by multiple factors.

Numerous studies have overcome this limitation by combining DO concentrations with stable oxygen isotopes (Levine et al., 2009; Mader et al., 2017; Li et al., 2019; Zhou et al., 2021; Piatka et al., 2022). The DO concentration, coupled with its oxygen isotopic composition, can provide additional information because it shows decoupling behaviors depending on oxygen sources and sink processes in the oxygen isotope and DO relationship (Levine et al., 2009; Zhou et al., 2021). For example, diagnosing the DO supply process in water with saturation reaching 100% may not be straightforward because surface waters at 100% saturation have been simultaneously influenced by both the equilibrium gas exchange with the atmosphere and photosynthesis. However, since photosynthesis produces DO with oxygen isotopic compositions similar to the oxygen isotopes in source water (approximately 0‰), they are lower than the $\delta^{18}O_{DO}$ of air-saturated water (24.2‰ with respect to the Vienna Standard Mean Ocean Water [VSMOW]). Thus, the corresponding $\delta^{18}O_{DO}$ values help provide new insights into the multiple components regarding 100% DO-saturated waters (Kroopnick and Craig, 1972; Parker et al., 2005). In addition, oxygen removal processes such as respiration and oxidation of metals can be differentiated from these DO supply processes by causing distinct shifts in the $\delta^{18}O_{DO}/[O_2]$ relationship, resulting from increasing $\delta^{18}O_{DO}$ values as DO decreases (Wassenaar and Hendry, 2007; Sutherland et al., 2018).

The center of the Ulleung Basin (UB) in the East/Japan Sea (EJS) has been in the spotlight due to the distinct DO consumption in the bottom layer. According to Kang et al. (2010), the vertical profiles of DO in the UB can be classified into three types. In general, surface water, where oxygen from the atmosphere is dissolved into the water and is produced via photosynthesis, is primarily affected by DO-supplying processes. As depth increases, decreases in DO are generally attributed to aerobic respiration, reaching the oxygen minimum zone between a few hundred meters and 1000 m deep. In the absence of available reductants (e.g., organic matter), DO concentration remains constant well below depths deeper than 1000 m (Kang et al., 2010; Gamo, 2011). However, the predominant distribution of DO in the center of the UB shows a distinctive structure with characteristic DO depletion in the bottom waters overlying the surface sediments (described as type 2 in Kang et al., 2010).

Compared with those of the other regions of the EJS, the surface sediments of the UB contain high organic carbon (>2.5% dry wt.; Cha et al., 2007; Lee et al., 2008), which is unusually high considering its bed depth of 2200 m. There are several studies supporting the high organic matter content in the sediments of the UB; the high organic matter content could result from organic carbon accumulation rates exceeding 2 g C m^{-2} $year^{-1}$ (Lee et al., 2008) associated with the combination of high export flux (*f*-ratio ≈ 0.28) of phytoplankton-derived labile organic carbon through enhanced primary production (Kwak et al., 2013) and lateral transport of resuspended organic matter that may be related to downslope currents along the continental slope (Yoo and Park, 2009; Hyun et al., 2017; Kim et al., 2017; Hahm et al., 2019; Lee et al., 2019; Hyun et al., 2022; Lee et al., 2022). In general, the degradation of excess organic matter in bottom waters near sediments significantly influences DO concentrations and its $\delta^{18}O_{DO}$ (Wassenaar and Hendry, 2007; Zhou et al., 2021). Some studies have reported that excess dissolved Fe and Mn via sediment redox processes are highly active in the sediments of the UB (Hyun et al., 2022; Seo et al., 2022). Furthermore, they are released into the water column, subsequently oxidized by oxygen, and settle in the sediment (Kim et al., 2017). Thus, the DO content of the bottom water layer in the UB can be determined by various sinks, such as microbial respiration, biodegradation and oxidation, and the oxidation of transitional metals because molecular oxygen is the most biogeochemically active oxidant (Lee et al., 2003). Ultimately, these environmental conditions can fuel oxygen consumption in the bottom water column. While there have been some studies supporting the intriguing distribution of DO observed in the bottom waters of the UB, these studies may translate DO consumption using indirect tracers, such as biogeochemical organic carbon cycles (Kim et al., 2017; Lee et al., 2022), benthic biological activity (Hyun et al., 2022), and nutrients (Kim et al., 2012).

Several studies have concluded that $\delta^{18}O_{DO}$, in addition to DO concentrations, is best used as a direct diagnostic tool for the integrated processes influencing DO concentrations (Levine et al., 2009; Mader et al., 2017; Sutherland et al., 2018; Köhler et al., 2021) because the isotopic signature of DO is controlled by isotopic fractionation and relative rates through reactions with various reductants. This study aims to investigate the processes influencing the decline in DO concentrations observed in the bottom water of the UB. We present the first $\delta^{18}O_{DO}$ dataset for a distinctive DO depletion zone of the UB, collected over three years of field observations (2020–2022), and interpret DO consumption based on isotopic systematics because $\delta^{18}O_{DO}$ data could be a direct tracer for understanding DO controlling processes.

2 Materials and methods

2.1 Data and sample collection

The EJS, which is connected to the Pacific Ocean through shallow straits (depth< 150 m), the Korea-Tsushima Strait in the southwest and the Tsugaru Strait in the northeast, is a semi-enclosed marginal sea surrounded by the Korean Peninsula, Far

Eastern Eurasia, and the Japan Archipelago. It has a maximum depth of approximately 3800 m (an average depth of 1667 m) (Figure 1). Depending on a short timescale (approximately 100 years) of deep-water ventilation (Tsunogai et al., 1993; Kumamoto et al., 1998), the oxygen-rich surface water transports to deep layers of the ocean. The bottom topography of EJS is characterized by three relatively deep basins: the Japan Basin in the north, the Yamato Basin in the southeast, and the Ulleung Basin (UB) in the southwest (Figure 1).

Field measurements and seawater sampling were performed at the central area of the UB, Station E5, with a water depth of approximately 2150 m (Figure 1; 37°00´N, 131°00´E) during the three years of field campaigns from 2020 to 2022. Two cruises onboard the R/V *Isabu* were conducted in March 2020 and February 2022, and one onboard the R/V *Eardo* was in July 2021. Hydrographic properties, including water temperature, salinity, and turbidity (C-star transmissometer; path length 25 cm), were measured using a conductivity-temperature-depth (CTD) profiler (SBE 911plus; Sea-Bird Electronics) calibrated within 2 years from each cruise period except for transmissometer. DO profiles were obtained using a sensor (SBE 43; Sea-Bird Electronics), and all profiles were calibrated by Winkler titration. The *in situ* calibration procedure for each DO profile includes computing the correction factors (slope and intercept) based on the regression between Winkler and the DO sensor (Supplementary Figure 1; Kang and Kim, 2023). The CTD casting depth was determined to be approximately 10 m above the seafloor to acquire the hydrographic and chemical properties near the seawater–sediment interface as closely as possible.

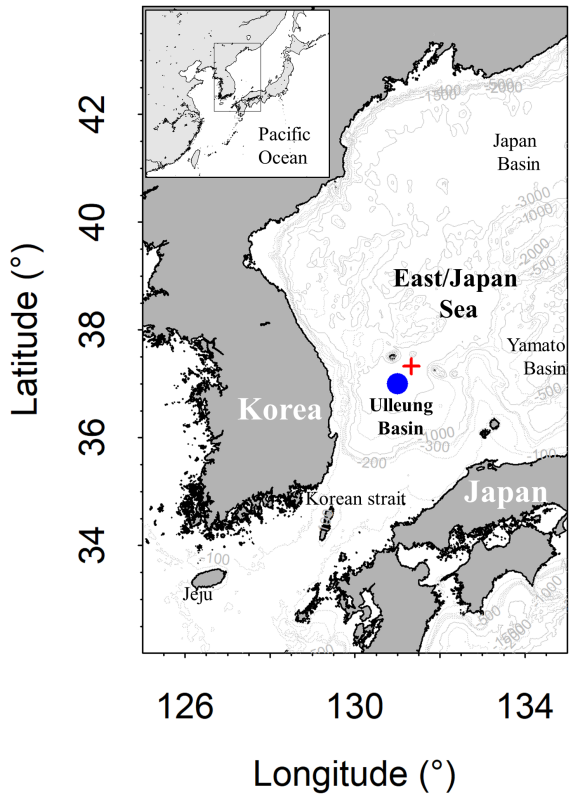

FIGURE 1
Map of the study area with bathymetric contours, showing the sampling (blue circle: E5; 37°00´N, 131°00´E) and mooring stations (red cross: EC1; 37°20´N, 131°20´E) of the Ulleung Basin of the East/Japan Sea.

Samples for the analyses of DO concentration and oxygen isotopic composition were collected using 12 L Niskin bottles attached to a carousel water sampler. Water sampling depths were determined based on the vertical profile of the DO sensor during each field campaign. To obtain gaseous samples for the oxygen isotope analysis of DO, the ultra-vacuum sample collection system designed by Emerson et al. (1991) was modified in this study (Figure 2). In particular, the most significant change from the previous system was that dissolved gases were extracted and collected directly in the field to inhibit the oxidation of dissolved metals and further biological activity (Köhler et al., 2020). A sample collection system consisting of two glass bottles attached via a Cajon Ultra-Torr connector was used to collect the mixture of gases from the seawater. The system was evacuated under high vacuum pressure (< 40 mTorr) using a vacuum preparation system to remove headspace gases from the bottles. Approximately 330 mL of seawater was carefully and slowly transferred to the bottom bottle. In the field, a mixture of dissolved gases, including oxygen, was immediately extracted from the seawater to the headspace of the bottom bottle. The stopcock of the top bottle was opened, and the extracted gases in the bottom bottle were equilibrated for approximately 15 min in the expanded headspace at room temperature. Subsequently, the stopcock of the top bottle, which was filled with the extracted dissolved gases, was closed, and the obtained samples were analyzed within five months to measure the oxygen isotopic composition of DO in the extracted gases.

2.2 Analysis of the concentration and oxygen isotope composition of DO

The DO concentrations of the seawater samples were determined following the high-precision Winkler method (precision of <0.7 μmol kg^{-1}) using an automatic photometric titrator (DOT-05, Kimoto Electric). The oxygen isotopic composition of DO was measured using the dual-inlet system of an isotope ratio mass spectrometer (IRMS; Thermo Scientific 253 Plus). A mixture of gases that were immediately extracted from the seawater was directly introduced into the sample reservoir of the dual-inlet system without gas separation (Abe and Yoshida, 2003), and only water vapor in the sample was removed by passing it through a molecular sieve 13X water trap. The samples and the reference (atmospheric air) were balanced to a common voltage, resulting in similar pressures within the IRMS. The oxygen isotopic composition of DO was reported in typical delta notation (hereafter $\delta^{18}O_{DO}$) and is expressed as $\delta^{18}O = [(X_{sample}/X_{standard}) - 1] \times 1000$ in parts per thousand (‰), where X is the ratio of the abundance of heavier (^{18}O) to lighter (^{16}O) isotopes. All results were calibrated and reported with respect to atmospheric O_2, using a value of +23.5‰ relative to the VSMOW (Kroopnick and Craig, 1972). The analytical precision, expressed as the standard deviation,

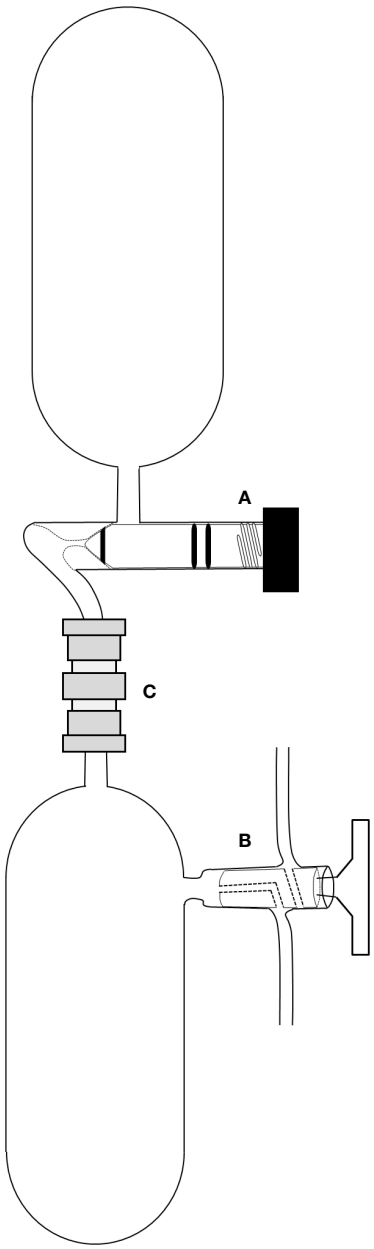

FIGURE 2
Schematic diagram of the sampling bottle set used to extract the dissolved gases from the seawater samples. The system consisting of the **(A)** top and **(B)** bottom bottles was connected by **(C)** a Cajon Ultra-Torr connector.

was better than 0.04‰ for $\delta^{18}O_{DO}$. The reproducibility of the two replicate measurements was better than 0.09‰ for $\delta^{18}O_{DO}$.

3 Results

Below 1000 m in the water column, temperature (0.18 ± 0.05°C) and salinity (34.06 ± 0.01) taken during our cruises were uniform, whereas the temperature and salinity in the upper ocean (<300 m) underwent seasonal changes (Supplementary Figure 2D). The vertical structures of the concentrations and oxygen isotopic composition ($\delta^{18}O_{DO}$) of DO were largely divided into several layers according to the various processes that added or removed oxygen from the water at different depths. Overall, the $\delta^{18}O_{DO}$ profiles show an opposite distribution compared with the DO profiles (Figure 3). In Figure 3A, DO concentrations from the surface to 300 m over the 3 years of field campaigns showed consistently high concentrations (256.5 ± 11.9 μmol kg^{-1}, mean ± SD); whereas DO concentrations for 2020 and 2022 ranged from 247 μmol kg^{-1} to 273 μmol kg^{-1} and from 239 μmol kg^{-1} to 275 μmol kg^{-1}, respectively. DO concentrations exhibited relatively large variation in July 2021, ranging from 214 μmol kg^{-1} to 276 μmol kg^{-1}. Surface water showed low $\delta^{18}O_{DO}$ values. With decreasing DO concentrations, $\delta^{18}O_{DO}$ increased up to approximately 32.3‰ in 2020 and 2022 and showed a maximum of 33.5‰ in 2021 at depths of 750–1000 m (Figure 3B).

The oxycline depth of each field campaign was observed at a similar depth range between 300 and 1000 m, where DO gradually decreased by approximately 193 μmol kg^{-1} (at least 55–56% DO saturation) while $\delta^{18}O_{DO}$ increased to approximately 4.5‰ with depth. Below a depth of 1000 m, low DO concentrations of < 199 μmol kg^{-1} were usually observed, which showed small declines up to a depth of 1800 m (maximum of 3 μmol kg^{-1}). From a depth of 1000–1800 m, $\delta^{18}O_{DO}$ values also seem to decrease. In this zone, the vertical patterns of each DO profile collected during the three cruises are not notably different; however DO concentrations in 2021 and 2022 were slightly lower than those in 2020 (approximately 5.0 μmol kg^{-1}). In this study, the difference in DO concentration among three independent profiles observed at same station (Figure 3A) was not considered based on the large variability of DO times-series data of mooring; DO concentrations have fluctuated by more than 5 μmol kg^{-1} at 1400 m and by approximately 10 μmol kg^{-1} at 2250 m over the time (Supplementary Figure 3).

Compared with a depth range of 1000–1800 m, the DO concentration declined relatively sharply from 1800 m to the bottom depth (2146 m). Within this bottom layer, the total magnitude of decrease was 4–5 μmol kg^{-1}. In particular, in 2020, the DO concentration continued to decline toward the bottom depth from 197.3 to 193.3 μmol kg^{-1}. The DO in 2021 and 2022 began declining more rapidly in the deeper water layer (approximately 1900 m) than in 2020 and then indicated a gentle decrease or no marked decline (Figure 3A). Although there was a slight difference in the depletion patterns from year to year, a substantial decrease in DO at the bottom boundary layer was consistently observed over all field observations. In this DO depletion zone, the $\delta^{18}O_{DO}$ indicated low values compared with the upper layers (< 1800 m). They decreased gradually from 1000 m to the bottom depth (approximately 0.5–2.0‰). Actually, the decreasing change in $\delta^{18}O_{DO}$ can be observed in the depth range of approximately 1000 to 2146 m. Our focus was the discontinuity in the DO profile of the bottom layer. This water layer exhibited relatively steep oxygen gradients and low $\delta^{18}O_{DO}$ over a few hundred meters of depth compared with a depth range of 1000–1800 m, as illustrated in Figure 3.

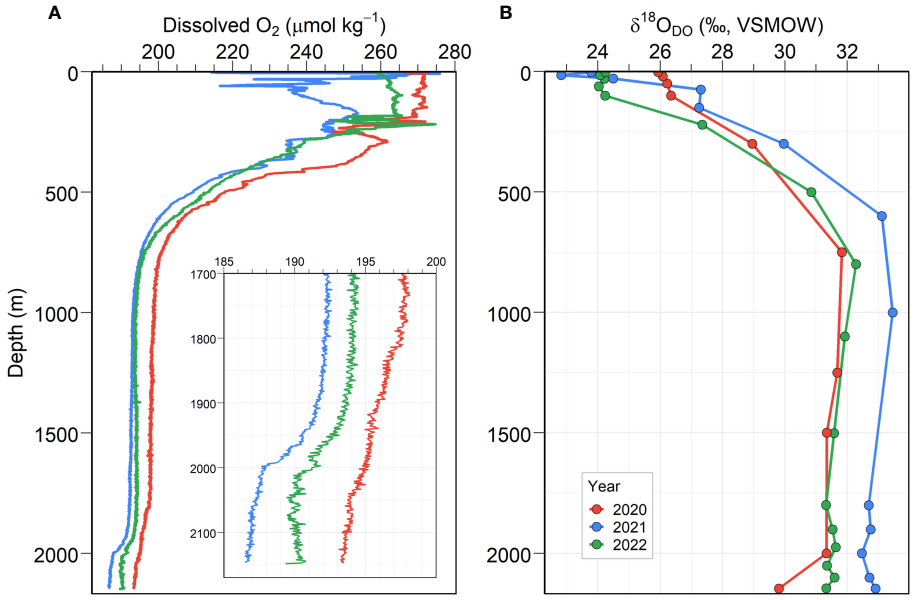

FIGURE 3
Vertical structures of the **(A)** DO concentrations and **(B)** $\delta^{18}O_{DO}$ collected during the 3 years of field campaigns in the UB.

4 Discussion

4.1 Potential processes driving DO depletion

At the center of the UB, DO concentrations decrease monotonously up to 1000 m through the decomposition of organic matter, which primarily settles from the surface waters. Thus, the oxygen consumption rate is high in the oxycline and then decreases with depth (Feely et al., 2004; Karstensen et al., 2008). As $^{16}O_2$ was preferentially consumed during respiration, following a mass-dependent law, the residual DO became progressively enriched in ^{18}O (i.e., $\delta^{18}O_{DO}$ increase). However, our results show the occurrence of ^{18}O-depleted DO, coinciding with the decrease in DO (4–5 μmol kg^{-1}) in the bottom layer of the UB observed in this study (Figures 3A, B). Therefore, we confirmed that different mechanisms contribute to the oxygen sinks of the bottom water column. The possibility of a mixing effect between different water masses could be ruled out as demonstrated in a previous study (Kang et al., 2010), because the straight lines appear in the T-S diagram (See insert of Supplementary Figure 2D).

To explain the DO depletion from 1800 m to the bottom of the UB, some studies have mentioned several physical and biogeochemical processes as possible DO sinks (Kang et al., 2010; Hyun et al., 2022). The magnitude of decrease in DO from 1800 m to 2146 m of the UB, as reported by some studies, was similar to the values reported in this study (4–5 μmol kg^{-1}) (Kang et al., 2010; Hyun et al., 2022). Kang et al. (2010) mentioned several possibilities of water mass intrusion affecting different aging rates and/or low-oxygenated water from the Japan Basin, denitrification, and aerobic respiration and finally concluded that organic matter decomposition in surface sediments play a crucial role in DO decrease in the bottom water layer of the UB. Hyun et al. (2022) demonstrated that bioactive dissolved organic matter derived from sediments stimulates heterotrophic microbial metabolism regarding the rapid expense of oxygen in the bottom water layer. Thus, to date, DO depletion in the bottom layer of the UB has been constrained as a result of respiratory DO consumption, which is closely related to environmental conditions caused by the high organic matter content in the surface sediment. Lee et al. (2022) noted that depending on the overall environmental conditions of the surface sediment of the UB, the re-oxidation of reduced elements (i.e., Mn^{2+}, Fe^{2+}, NH^{+}, and H_2S), as well as the oxidation of organic carbon, could contribute to the sediment oxygen consumption rate. Lee et al. (2022) did not mention the distribution of DO in the water column; however, it is thought that the oxygen consuming processes in the bottom waters in contact with sediments will not differ significantly from the sediment oxygen consumption processes. Ultimately, this study focused on three possible DO-consuming processes in the bottom water: (1) respiration (i.e., the decomposition of organic matter and/or microbial respiration), (2) mineral oxidation, and (3) diffusive transport from a highly oxygenated water column into oxygen-depleted sediments. Logically, these processes could be fully explained by unique local biogeochemical events related to the high organic matter content in the surface sediments of the UB and the presence of a deep nepheloid layer that causes interactions between the water column and sediments (Supplementary Figure 2C). Therefore, the interaction between the bottom water and surface sediments should be considered a crucial factor affecting the distribution of DO in the study area. First, sediment resuspension that may be stimulated by near-bottom currents (Chang et al., 2009; Kim et al., 2013) and lateral transport (Lee et al., 2019) in the bottom layer of the UB can form the nepheloid

layer and enable the reintroduction of deposited organic matter into the water column. Moreover, within the nepheloid layers, some evidence proves the behavior of reduced elements, such as dissolved Fe and Mn, released from sediments (e.g., Seo et al., 2022). Previous studies have reported that dissolved Fe and Mn, which are redox-sensitive trace elements (Stumm and Morgan, 1996), show higher concentrations in sediments as well as the water column of the UB than in those of other basins (Cha et al., 2007; Hyun et al., 2017). Thus, depending on the oxygenated-depth of only a few millimeters in surface sediments of the UB (Hyun et al., 2017; Lee et al., 2022), the release of dissolved Fe and Mn from anoxic-sediments into the water column overlying the bottom can occur because Fe and Mn oxides are used as oxidants for the degradation of organic matter in sediments (Kim and Kim, 2016; Kim et al., 2017; Seo et al., 2022), which then oxidizes into a solid phase owing to the interaction with DO. In addition, the diffusion of DO from oxic-water into surface sediments could explain the occurrence of a DO-depleted bottom layer (Wassenaar and Hendry, 2007; Li et al., 2019).

4.2 ^{18}O-depletion in the bottom layer

To postulate the DO consumption processes that contribute to DO depletion in the bottom waters of the UB, we explored the oxygen isotopic behaviors derived from the DO consumption processes using $\delta^{18}O_{DO}$ and the DO saturation degree ($[O_2]_t/[O_2]_i$) relationship (Rayleigh distillation equation; Aggarwal et al., 1997; Nakayama et al., 2007). The isotopic signature of DO is controlled by the isotopic fractionation factor of the potential O_2 consumption processes and their relative rates. The Rayleigh distillation equation was used to calculate the oxygen fractionation factor (α) of DO consumption (Aggarwal et al., 1997; Nakayama et al., 2007).

$$\alpha = 1 + \frac{\delta^{18}_t - \delta^{18}_i}{10^3 ln([O_2]_t/[O_2]_i)} \quad (1)$$

where δ^{18}_i and δ^{18}_t are the isotopic compositions of the initial and residual DO at the time t, respectively, and $[O_2]_t$ is the residual DO concentration. It was assumed that $[O_2]_i$ was equal to the saturation O_2 concentration at the temperature and salinity of a given water sample. The observed $\delta^{18}O_{DO}$ versus $\ln([O_2]_t/[O_2]_i)$ was plotted in Figure 4. The fractionation factor (α) for oxygen consumption processes was calculated using Equation (1) by applying the δ^{18}_i value for 24.2‰ (at $\ln([O_2]_t/[O_2]_i)=0$) in equilibrium with the atmosphere (Bender and Grande, 1987). The equilibrium value of 24.2‰ at 25°C (Kroopnick and Craig, 1972) has been adapted as the initial δ^{18} (δ^{18}_i) because $\delta^{18}O_{DO}$ starting point (24.2‰) of oxygen entering the water column from the atmosphere can be changed by biological processes such as respiration and mineral interaction.

Conventional knowledge, depending on respiration, is that the corresponding $\delta^{18}O_{DO}$ should result in an increase as $\ln([O_2]_t/[O_2]_i)$ decreases (Bender, 1990; Kiddon et al., 1993; Angert and Luz, 2001; Levine et al., 2009). In practice, the monotonic and opposite pattern between $\ln([O_2]_t/[O_2]_i)$ (i.e., the decrease from 0 to –0.5) and $\delta^{18}O_{DO}$ (i.e., the increase from 26‰ to 33.5‰) was observed continuously from 100 m to the end of the oxycline zone (approximately 1000 m) (Figure 4A). The α values for DO consumption closely relative to the respiration determined in the literature ranged from 0.981 to 0.992 (the isotopic effect of –20 to –10‰) (Bender, 1990; Wassenaar and Hendry, 2007; Sutherland et al., 2018). The only study to date, by Nakayama et al. (2007), reported a respiratory O_2 consumption fractionation factor of 0.987 for the waters from 298 to 3584 m (bottom depth of 3643 m) in the other basin of the EJS (i.e., 41° 21.20′N, 137°20.06′N). Similarly, the regression line of the Rayleigh distillation equation yielded an isotopic effect with α values of 0.986, 0.984, and 0.986 in 2020, 2021, and 2022, respectively. Therefore, the $\delta^{18}O_{DO}$ values in the mesopelagic layer of the UB agree well with the assumptions regarding O_2 consumption through respiration.

In contrast, our result, that $\ln([O_2]_t/[O_2]_i)$ and $\delta^{18}O_{DO}$ in the depth range of approximately 1000 to 2146 m of the UB showed a

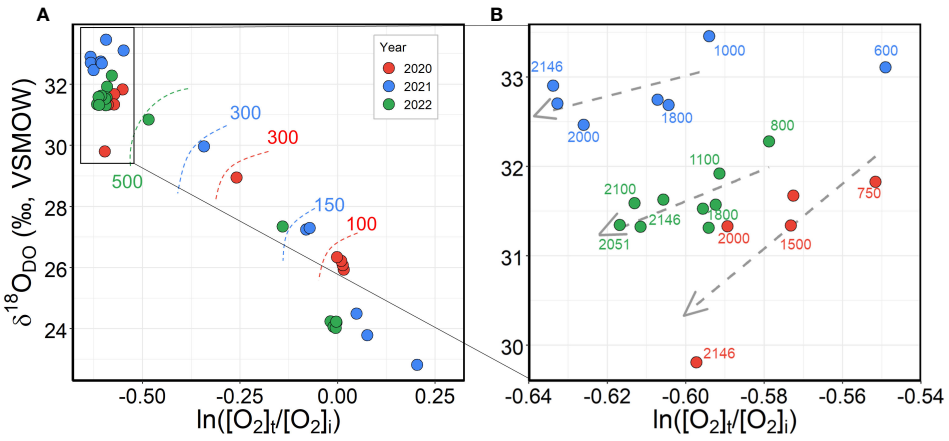

FIGURE 4
Plots of the observed $\delta^{18}O_{DO}$ versus the DO saturation degree ($\ln([O_2]_t/[O_2]_i)$) for water column **(A)** from the surface water to bottom water and **(B)** from 1000 m to the bottom water, where $[O_2]_t$ is the residual O_2 saturation, and $[O_2]_i$ is the O_2 saturation at 100%. The points denote data collected during the 3 years of field campaigns in the UB. The depths are marked around each point.

simultaneous apparent decrease for 0.03 ± 0.007 and 1.32 ± 0.61‰, respectively (Figure 4B), defies conventional knowledge regarding respiratory O_2 consumption in the water column. The $\delta^{18}O_{DO}$ values indicated an inverse isotopic behavior of respiration. From this discontinuity below the mesopelagic layer caused by unexpected ^{18}O-depleted dissolved oxygen, we postulate that the corresponding $\delta^{18}O_{DO}$ in the bottom waters may be controlled by independent isotopic fractionation resulting from different DO-consuming mechanisms. In the previous section, as potential processes driving DO depletion, the respiration, mineral oxidation, and diffusive transport to anoxic sediment can lead to DO depletion in the bottom layer of the UB, which is experienced by local physicochemical properties, such as the resuspension of organic matter and the release of reduced minerals from surface sediments in the nepheloid layers. According to a mass-dependent law, these processes –respiration, oxidation of metals such as Mn and Fe (Wassenaar and Hendry, 2007; Oba and Poulson, 2009a; Oba and Poulson, 2009b; Sutherland et al., 2018), and diffusion (Clark and Fritz, 1997; Lee et al., 2003; Wassenaar and Hendry, 2007)–increase $\delta^{18}O_{DO}$ in the residual DO (namely, light isotopes are preferentially oxidized and/or transported). If each of these DO sink processes can be identified by a unique α value, then it may provide insight into the multicomponent progression of DO consumption. Based on this assumption, we theorized about the multiple DO consumptions in the bottom water of the UB based on oxygen isotopic fractionation (Figure 5). Starting from the air-saturated surface to the bottom depth (approximately 2146 m; Point A), the slope of the regression line was slightly different from that calculated for the mesopelagic layer (Point B) where respiration dominates. The estimated α values for 2020, 2021, and 2022 in the bottom water were relatively larger (0.991, 0.986, and 0.988, respectively) (mean value of 0.988 ± 0.001) than those in the mesopelagic layer. We believe that this large α is due to the contribution of other DO sinks, together with respiration to DO consumption. In contrast to the diffusive transport of DO (α_d = 0.986; Clark and Fritz, 1997), mineral oxidation has a large fractionation factor ($\alpha_o > \alpha_r$) that distinguishes it from respiration (Wassenaar and Hendry, 2007). Ultimately, larger α values estimated in the bottom waters could be derived from the oxidation of minerals such as Mn and Fe because the impacts of mineral oxidation result in α_o, which is less fractionating than that for respiration (Taylor et al., 1984; Kiddon et al., 1993; Lee et al., 2003; Oba and Poulson, 2009b). Therefore, the α_m value in the bottom layer reported in this study represents the net fractionation factor produced by combining multiple DO consumption processes (Figure 5). As depicted in Figure 5, from 1000 m to 2146 m, the tendency of $\delta^{18}O_{DO}$ to decrease (Figure 3B) could be interpreted as a result of mixing between distinguishable DO-consuming processes: multiple DO-consuming processes in the bottom layer (referred to as Point A) and water column respiration in the mesopelagic layer (referred to as Point B).

In addition, our results indicate that the contribution of the various consumption processes to the total DO consumption at the bottom layer is dynamic and non-stationary. Therefore, the calculated α_r and α_m values for individual field observations are slightly different (Figure 4); however, larger value of α_m than α_r is consistent during all cruises. Unfortunately, it is not feasible to accurately quantify and/or fractionate multiple processes of DO consumption. Nevertheless, our work here emphasizes the need to consider the contribution of mineral oxidation to total DO consumption when studying the oxygen consumption mechanism

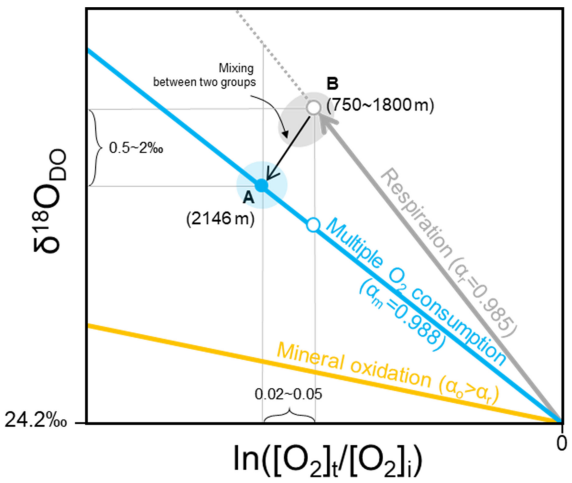

FIGURE 5
Theoretical schematic of $\delta^{18}O_{DO}$ versus $\ln([O_2]_t/[O_2]_i)$, showing the consumptive oxygen isotope fractionation factors. Highly exaggerated straight lines in grey and blue indicate the averaged fractionation factors of 0.985 ± 0.001 (α_r; water column respiration) and 0.988 ± 0.002 (α_m; multiple DO-consuming processes), respectively. The averaged values of fractionation factor indicated on lines were calculated from the data obtained during the field campaigns, starting with the identified $\delta^{18}O_{DO}$ of air-saturated water (24.2‰). Points A and B denote the end-points of bottom water and mesopelagic layer, respectively. The yellow line depicted represents the fractionation factor for mineral oxidation (α_o), which was undoubtedly larger than that for respiration. However, an exact value cannot be specified in this study.

in the bottom layer of the UB. We could maintain our assertion that mineral oxidation contributes to a certain extent of DO consumption in the bottom layer through a simple stoichiometry of Mn oxidation ($Mn^{2+}+0.5O_{2(aq)}+H_2O \Leftrightarrow MnO_{2(s)}+2H^+$). The decreased DO (approximately 4–5 μmol/kg) is comparable to the maximum oxygen demand (5 μM) estimated by Mn^{2+} concentration reported by Hyun et al. (2017) (approximately 10 μM in the uppermost layer of sediment).

5 Conclusions

Considering the high concentration of DO in the bottom waters of the UB, the high organic contents in the surface sediments are exceptional. Furthermore, oxygen is depleted within just a few millimeters of the sediments, and the excess dissolved Fe and Mn, via sediment redox processes, are highly active, subsequently being released into waters above the sediments. In these unique environmental settings of the UB, where such conditions are scarcely found elsewhere in the oceans, explaining the remarkable decrease in DO in the bottom layer is complicated because multiple DO-consuming processes can co-occur sufficiently. In this study, we report the first $\delta^{18}O_{DO}$ measurements, together with DO concentrations to delineate oxygen isotope fractionation for the sum of multiple factors influencing DO depletion in the bottom layer of the UB. The vertical structures of DO observed in our cruise campaigns showed a typical decline in the mesopelagic layer, but an unforeseen decrease in DO concentrations in the bottom layer. Moreover, $\delta^{18}O_{DO}$ also decreased continuously with depth in the bottom layer. Subsequently, we found an unexpected negative shift in $\delta^{18}O_{DO}$ with decreasing DO concentration in the bottom layer of the UB. We attribute the decrease in $\delta^{18}O_{DO}$ to the net effect of the consumptive isotopic fractionation of multiple processes that respiration, mineral oxidation, and molecular diffusion to sediments co-occur. In particular, the DO consumption process responsible for the ^{18}O depletion could be identified based on the isotopic fractionation of mineral oxidation. The behavior of reduced minerals in the bottom layer reported previously strengthens our findings. We demonstrate that oxygen consumption mechanisms in natural environments can be discriminated using different isotope fractionation factors during DO consumption. This study must be regarded as the first attempt to constrain the multiple oxygen consumption processes in the bottom waters of the UB based on isotopic signatures as a direct tracer. Further experimental studies are needed to improve the understanding of isotopic fractionation during DO consumption and characterize the proportion associated with each individual and specific DO-consuming reaction. Nevertheless, the net fractionation factors (α_m) proposed in this study can serve as a useful indicator for elucidating the complex processes responsible for oxygen consumption mechanisms in marine environments.

Data availability statement

The original contributions presented in the study are included in the article/Supplementary Material. Further inquiries can be directed to the corresponding author.

Author contributions

YK: Data curation, Formal Analysis, Investigation, Methodology, Software, Validation, Visualization, Writing – original draft. D-JK: Conceptualization, Funding acquisition, Investigation, Methodology, Supervision, Writing – review & editing.

Funding

The author(s) declare financial support was received for the research, authorship, and/or publication of this article. This research was supported by the Korea Institute of Ocean Science and Technology (KIOST) (PEA0111).

Acknowledgments

We thank captains and all crew members of the R/V *Isabu* and *Eardo* of the Korea Institute of Ocean Science and Technology (KIOST) for the assistance with sampling campaigns.

Conflict of interest

The authors declare that the research was conducted in the absence of any commercial or financial relationships that could be construed as a potential conflict of interest.

Publisher's note

Supplementary material

The Supplementary Material for this article can be found online at: https://www.frontiersin.org/articles/10.3389/fmars.2023.1276028/full#supplementary-material

References

Abe, O., and Yoshida, N. (2003). Partial pressure dependency of $^{17}O/^{16}O$ and $^{18}O/^{16}O$ of molecular oxygen in the mass spectrometer. *Rapid Commun. Mass Spectrom.* 17, 395–400. doi: 10.1002/rcm.923

Aggarwal, P. K., Fuller, M. E., Gurgas, M. M., Manning, J. F., and Dillon, M. A. (1997). Use of stable oxygen and carbon isotope analyses for monitoring the pathways and rates of intrinsic and enhanced in *situ* biodegradation. *Environ. Sci. Technol.* 31, 590–596. doi: 10.1021/es960562b

Angert, A., and Luz, B. (2001). Fractionation of oxygen isotopes by root respiration: Implications for the isotopic composition of atmospheric O_2. *Geochim. Cosmochim. Acta* 65, 1695–1701. doi: 10.1016/S0016-7037(01)00567-1

Bender, M. L. (1990). The $\delta^{18}O$ of dissolved O_2 in seawater: A unique tracer of circulation and respiration in the deep sea. *J. Geophys Res: Oceans* 95, 22243–22252. doi: 10.1029/JC095iC12p22243

Bender, M. L., and Grande, K. D. (1987). Production, respiration, and the isotope geochemistry of O_2 in the upper water column. *Glob. Biogeochem. Cycles* 1, 49–59. doi: 10.1029/GB001i001p00049

Bocaniov, S. A., Schiff, S. L., and Smith, R. E. (2012). Plankton metabolism and physical forcing in a productive embayment of a large oligotrophic lake: insights from stable oxygen isotopes. *Freshw. Biol.* 57 (3), 481–496. doi: 10.1111/j.1365-2427.2011.02715.x

Cha, H. J., Choi, M. S., Lee, C. B., and Shin, D. H. (2007). Geochemistry of surface sediments in the southwestern East/Japan Sea. *J. Asian Earth Sci.* 29, 685–697. doi: 10.1016/J.JSEAES.2006.04.009

Chang, K. I., Kim, K., Kim, Y. B., Teague, W. J., Lee, J. C., and Lee, J. H. (2009). Deep flow and transport through the Ulleung Interplain Gap in the southwestern East/Japan Sea. *Deep Sea Res. I: Oceanogr. Res. Pap.* 56, 61–72. doi: 10.1016/j.dsr.2008.07.015

Clark, I. D., and Fritz, P. (1997). *Environmental isotopes in hydrogeology* (New York: Lewis Publishers). doi: 10.1201/9781482242911

Emerson, S., Quay, P., Stump, C., Wilbur, D., and Knox, M. (1991). O_2, Ar, N_2, and ^{222}Rn in surface waters of the subarctic ocean: Net biological O_2 production. *Glob. Biogeochem. Cycles* 5, 49–69. doi: 10.1029/90GB02656

Feely, R. A., Sabine, C. L., Schlitzer, R., Bullister, J. L., Mecking, S., and Greeley, D. (2004). Oxygen utilization and organic carbon remineralization in the upper water column of the Pacific Ocean. *J. Oceanogr.* 60, 45–52. doi: 10.1023/B:JOCE.0000038317.01279.aa

Gamo, T. (2011). Dissolved oxygen in the bottom water of the Sea of Japan as a sensitive alarm for global climate change. *TrAC Trends Anal. Chem.* 30, 1308–1319. doi: 10.1016/j.trac.2011.06.005

Hahm, D., Rhee, T. S., Kim, H. C., Jang, C. J., Kim, Y. S., and Park, J. H. (2019). An observation of primary production enhanced by coastal upwelling in the southwest East/Japan Sea. *J. Mar. Syst.* 195, 30–37. doi: 10.1016/j.jmarsys.2019.03.005

Hanson, P. C., Carpenter, S. R., Kimura, N., Wu, C., Cornelius, S. P., and Kratz, T. K. (2008). Evaluation of metabolism models for free-water dissolved oxygen methods in lakes. *Limnol. Oceanogr.-Meth.* 6 (9), 454–465.

Hobbs, J.-P. A., and McDonald, C. A. (2010). Increased seawater temperature and decreased dissolved oxygen triggers fish kill at the Cocos (Keeling) Islands, Indian Ocean. *J. Fish Biol.* 77, 1219–1229. doi: 10.1111/j.1095-8649.2010.02726.x

Hyun, J. H., Kim, B., Han, H., Baek, Y. J., Lee, H., Cho, H., et al. (2022). Sediment-derived dissolved organic matter stimulates heterotrophic prokaryotes metabolic activity in overlying deep sea in the Ulleung Basin, East Sea. *Front. Mar. Sci.* 448. doi: 10.3389/fmars.2022.826592

Hyun, J. H., Kim, S. H., Mok, J. S., Cho, H., Lee, T., Vandieken, V., et al. (2017). Manganese and iron reduction dominate organic carbon oxidation in surface sediments of the deep Ulleung Basin, East Sea. *Biogeosciences* 14, 941–958. doi: 10.5194/bg-14-941-2017

Joos, F., Plattner, G.-K., Stocker, T. F., Körtzinger, A., and Wallace, D. W. R. (2003). Trends in marine dissolved oxygen: Implications for ocean circulation changes and the carbon budget. *Eos Trans. AGU* 84 (21), 197–201. doi: 10.1029/2003EO210001

Kang, D. J., and Kim, Y. (2023). *In-situ* calibration of membrane type dissolved oxygen sensor for CTD. *Sea: J. Korean Soc Oceanogr.* 28, 41–50. doi: 10.7850/jkso.2023.28.1.041

Kang, D. J., Kim, Y. B., and Kim, K. R. (2010). Dissolved oxygen at the bottom boundary layer of the Ulleung Basin, East Sea. *Ocean Polar Res.* 32, 439–448. doi: 10.4217/OPR.2010.32.4.439

Karstensen, J., Stramma, L., and Visbeck, M. (2008). Oxygen minimum zones in the eastern tropical Atlantic and Pacific oceans. *Prog. Oceanogr.* 77, 331–350. doi: 10.1016/j.pocean.2007.05.009

Kiddon, J., Bender, M. L., Orchardo, J., Caron, D. A., Goldman, J. C., and Dennett, M. (1993). Isotopic fractionation of oxygen by respiring marine organisms. *Glob. Biogeochem. Cycles* 7, 679–694. doi: 10.1029/93GB01444

Kim, I. N., Min, D. H., and Lee, T. (2012). Deep nitrate deficit observed in the highly oxygenated east/Japan sea and its possible cause. *Terr. Atmospheric Ocean. Sci.* 23, 671–683. doi: 10.3319/TAO.2012.08.11.01(Oc)

Kim, J., and Kim, G. (2016). Significant anaerobic production of fluorescent dissolved organic matter in the deep East Sea (Sea of Japan). *Geophys. Res. Lett.* 43, 7609–7616. doi: 10.1002/2016GL069335

Kim, M., Hwang, J., Rho, T., Lee, T., Kang, D. J., Chang, K. I., et al. (2017). Biogeochemical properties of sinking particles in the southwestern part of the East Sea (Japan Sea). *J. Mar. Syst.* 167, 33–42. doi: 10.1016/j.jmarsys.2016.11.001

Kim, Y. B., Chang, K. I., Park, J. H., and Park, J. J. (2013). Variability of the dokdo abyssal current observed in the Ulleung Interplain Gap of the East/Japan Sea. *Acta Oceanol. Sin.* 32, 12–23. doi: 10.1007/s13131-013-0263-y

Köhler, I., Martinez, R. E., Piatka, D., Herrmann, A. J., Gallo, A., Gehringer, M. M., et al. (2021). How are oxygen budgets influenced by dissolved iron and growth of oxygenic phototrophs in an iron-rich spring system? Initial results from the Espan Spring in Fürth, Germany. *Biogeosciences* 18, 4535–4548. doi: 10.5194/bg-18-4535-2021

Köhler, I., Piatka, D., Barth, J. A., and Martinez, R. E. (2020). Beware of effects on isotopes of dissolved oxygen during storage of natural iron-rich water samples: A technical note. *Rapid Commun. Mass Spectrom.* 35, e9024. doi: 10.1002/rcm.9024

Kroopnick, P., and Craig, H. (1972). Atmospheric oxygen: isotopic composition and solubility fractionation. *Science* 175, 54–55. doi: 10.1126/science.175.4017.54

Kumamoto, Y. I., Yoneda, M., Shibata, Y., Kume, H., Tanaka, A., Uehiro, T., et al. (1998). Direct observation of the rapid turnover of the Japan Sea bottom water by means of AMS radiocarbon measurement. *Geophys. Res. Lett.* 25, 651–654. doi: 10.1029/98GL00359

Kwak, J. H., Hwang, J., Choy, E. J., Park, H. J., Kang, D. J., Lee, T., et al. (2013). High primary productivity and f-ratio in summer in the Ulleung basin of the East/Japan Sea. *Deep Sea Res. I: Oceanogr. Res. Pap.* 79, 74–85. doi: 10.1016/j.dsr.2013.05.011

Lee, E. S., Birkham, T. K., Wassenaar, L. I., and Hendry, M. J. (2003). Microbial respiration and diffusive transport of O_2, $^{16}O_2$, and $^{18}O^{16}O$ in unsaturated soils and geologic sediments. *Environ. Sci. Technol.* 37, 2913–2919. doi: 10.1021/es026146a

Lee, J. S., Han, J. H., An, S. U., Kim, S. H., Lim, D., Kim, D., et al. (2019). Sedimentary organic carbon budget across the slope to the basin in the southwestern Ulleung (Tsushima) Basin of the East (Japan) Sea. *J. Geophys. Res. Biogeosci.* 124, 2804–2822. doi: 10.1029/2019JG005138

Lee, D. K., Hong, G. H., Yamg, D. B., Kim, Y. I., and Seung-Hwan, M. (2022). Enhancement of sea surface chlorophyll a concentration by interaction of winds and currents in a cyclonic eddy in the Japan/east sea. *Ocean Sci. J.* 57 (2), 186–196. doi: 10.1007/s12601-022-00058-y

Lee, T., Hyun, J. H., Mok, J. S., and Kim, D. (2008). Organic carbon accumulation and sulfate reduction rates in slope and basin sediments of the Ulleung Basin, East/Japan Sea. *Geo-Mar. Lett.* 28, 153–159. doi: 10.1007/s00367-007-0097-8

Lee, J. S., Kim, S. H., Baek, J. W., Kim, K. T., Kim, D., Kim, Y. I., et al. (2022). Organic carbon oxidation in the sediment of the ulleung basin in the east sea. *J. Mar. Sci. Eng.* 10, 694. doi: 10.3390/jmse10050694

Levine, N. M., Bender, M. L., and Doney, S. C. (2009). The $\delta^{18}O$ of dissolved O_2 as a tracer of mixing and respiration in the mesopelagic ocean. *Glob. Biogeochem. Cycles* 23, GB1006. doi: 10.1029/2007GB003162

Li, B., Yeung, L. Y., Hu, H., and Ash, J. L. (2019). Kinetic and equilibrium fractionation of O_2 isotopologues during air-water gas transfer and implications for tracing oxygen cycling in the ocean. *Mar. Chem.* 210, 61–71. doi: 10.1016/j.marchem.2019.02.006

Mader, M., Schmidt, C., Geldern, R., and Barth, J. A. C. (2017). Dissolved oxygen in water and its stable isotope effects: A review. *Chem. Geol.* 473, 10–21. doi: 10.1016/j.chemgeo.2017.10.003

Nakayama, N., Obata, H., and Gamo, T. (2007). Consumption of dissolved oxygen in the deep Japan Sea, giving a precise isotopic fractionation factor. *Geophys. Res. Lett.* 34, L20604. doi: 10.1029/2007GL029917

Oba, Y., and Poulson, S. R. (2009a). Oxygen isotope fractionation of dissolved oxygen during abiological reduction by aqueous sulfide. *Chem. Geol.* 268, 226–232. doi: 10.1016/j.chemgeo.2009.09.002

Oba, Y., and Poulson, S. R. (2009b). Oxygen isotope fractionation of dissolved oxygen during reduction by ferrous iron. *Geochim. Cosmochim. Acta* 73, 13–24. doi: 10.1016/j.gca.2008.10.012

Parker, S. R., Poulson, S. R., Gammons, C. H., and DeGrandpre, M. D. (2005). Biogeochemical controls on diel cycling of stable isotopes of dissolved O_2 and dissolved inorganic carbon in the Big Hole River, Montana. *Environ. Sci. Technol.* 39, 7134–7140. doi: 10.1021/es0505595

Piatka, D. R., Venkiteswaran, J. J., Uniyal, B., Kaule, R., Gilfedder, B., and Barth, J. A. (2022). Dissolved oxygen isotope modelling refines metabolic state estimates of stream ecosystems with different land use background. *Sci. Rep.* 12, 10204. doi: 10.1038/s41598-022-13219-9

Seo, H., Kim, G., Kim, T., Kim, I., Ra, K., and Jeong, H. (2022). Trace elements (Fe, Mn, Co, Cu, Cd, and Ni) in the East Sea (Japan Sea): Distributions, boundary inputs, and scavenging processes. *Mar. Chem.* 239, 104070. doi: 10.1016/j.marchem.2021.104070

Stumm, W., and Morgan, J. J. (1996). *Aquatic Chemistry: Chemical Equilibria and Rates in Natural Waters*. (New York, NY: John Wiley & Sons).

Sutherland, K. M., Wankel, S. D., and Hansel, C. M. (2018). Oxygen isotope analysis of bacterial and fungal manganese oxidation. *Geobiology* 16, 399–411. doi: 10.1111/gbi.12288

Taylor, B. E., Wheeler, M. C., and Nordstrom, D. K. (1984). Stable isotope geochemistry of acid mine drainage: Experimental oxidation of pyrite. *Geochim. Cosmochim. Acta* 48, 2669–2678. doi: 10.1016/0016-7037(84)90315-6

Tsunogai, S., Watanabe, Y. W., Harada, K., Watanabe, S., Saito, S., and Nakajima, M. (1993). Dynamics of the Japan Sea deep water studied with chemical and radiochemical tracers. *Elsevier oceanogr. Ser.* 59, 105–119. doi: 10.1016/S0422-9894(08)71321-7

Wassenaar, L. I., and Hendry, M. J. (2007). Dynamics and stable isotope composition of gaseous and dissolved oxygen. *Groundwater* 45, 447–460. doi: 10.1111/j.1745-6584.2007.00328.x

Yoo, S., and Park, J. (2009). Why is the southwest the most productive region of the East Sea/Sea of Japan? *J. Mar. Syst.* 78, 301–315. doi: 10.1016/j.jmarsys.2009.02.014

Zhou, J., Zhu, Z. Y., Hu, H. T., Zhang, G. L., and Wang, Q. Q. (2021). Clarifying water column respiration and sedimentary oxygen respiration under oxygen depletion off the Changjiang estuary and adjacent East China Sea. *Front. Mar. Sci.* 7. doi: 10.3389/fmars.2020.623581d

Zuo, J., Song, J., Yuan, H., Li, X., Li, N., and Duan, L. (2019). Impact of Kuroshio on the dissolved oxygen in the East China Sea region. *J. Ocean. Limnol.* 37, 513–524. doi: 10.1007/s00343-019-7389-5